IRIS AperTO

UNIVERSITÀ DEGLI STUDI DI TORINO

AperTO - Archivio Istituzionale Open Access dell'Università di Torino

Cell death and neurodegeneration in the postnatal development of cerebellar vermis in normal and Reeler mice

This is the author's manuscript

Original Citation:

Availability:

This version is available http://hdl.handle.net/2318/1564147 since 2019-01-08T15:12:57Z

Published version:

DOI:10.1016/j.aanat.2016.01.010

Terms of use:

Open Access

Anyone can freely access the full text of works made available as "Open Access". Works made available under a Creative Commons license can be used according to the terms and conditions of said license. Use of all other works requires consent of the right holder (author or publisher) if not exempted from copyright protection by the applicable law.

(Article begins on next page)

18 April 2024

ACCEPTED MANUSCRIPT

Cell death and neurodegeneration in the postnatal development of cerebellar vermis in normal and *Reeler* mice

Claudia Castagna, Adalberto Merighi, Laura Lossi

University of Turin, Department of Veterinary Sciences
Postal address:

Largo Braccini, 2, I-10095 GRUGLIASCO (TO) Italy, EU
e-mail: claudia.castagna@unito.it

Short title: Apoptosis and autophagy in Reeler cerebellum

Accepted Manuscript

ACCEPTED MANUSCRIPT

Summary

Programmed cell death (PCD) was demonstrated in neurons and glia in normal brain development, plasticity, and aging, but also in neurodegeneration. (Macro)autophagy, characterized by cytoplasmic vacuolization and activation of lysosomal hydrolases, and apoptosis, typically entailing cell shrinkage, chromatin and nuclear condensation, are the two more common forms of PCD. Their underlying intracellular pathways are partly shared and neurons can die following both modalities, according to the type of death-triggering stimulus.

Reelin is an extracellular protein necessary for proper neuronal migration and brain lamination. In the mutant Reeler mouse, its absence causes neuronal mispositioning, with a notable degree of cerebellar hypoplasia that was tentatively related to an increase in PCD. We have carried out an ultrastructural analysis on the occurrence and type of postnatal PCD affecting the cerebellar neurons in normal and Reeler mice. In the forming cerebellar cortex, PCD took the form of apoptosis or autophagy and mainly affected the cerebellar granule cells (CGCs). Densities of apoptotic CGCs were comparable in both mouse strains at P0-P10, while, in mutants, they increased to become significantly higher at P15. In WT mice the density of autophagic neurons did not display statistically significant differences in the time interval examined in this study, whereas it was reduced in Reeler in the P0-P10 interval, but increased at P15. Besides CGCs, the Purkinje neurons also displayed autophagic features in both WT and Reeler mice. Therefore, cerebellar neurons undergo different types of PCD and a Reelin deficiency affects the type and degree of neuronal death during postnatal development of the cerebellum.

Key words: Reeler, cerebellum, apoptosis, autophagy, ultrastructure, granule cells, mouse, development

Accepted Manuscript

ACCEPTED MANUSCRIPT

1. Introduction

During development, the embryonic nervous system undergoes a complex and highly regulated sequence of events resulting in the generation of all neurons and glial cells of the adult brain, spinal cord and peripheral nervous system. In laminar brain regions, such as the cerebral and cerebellar cortices, neurons perform long distance migration and extend their axons to make highly precise synaptic connections with targets. Genetic mutations, as well as insults of heterogeneous nature, that affect the ability of neural cells to perform these sequenced steps result in developmental arrest and may lead to death of the affected cells (Yamaguchi and Miura, 2015).

Reeler is the first described mouse cerebellar mutation (Falconer, 1951) but the mutated protein, named Reelin, was only discovered many years later (D'Arcangelo et al., 1995). The Reeler phenotype is characterized by typical alterations in gait ("reeling"), associated with the total absence of Reelin in the recessive homozygous mice ($reln^{-/-}$). Reelin is an extracellular matrix glycoprotein secreted during neurogenesis and represents the first molecule of a complex intracellular cascade regulating neuronal migration (D'Arcangelo and Curran, 1998; Lambert de Rouvroit and Goffinet, 1998). The absence of Reelin induces anatomical anomalies in a large number of different areas of the central nervous system (CNS), including the olfactory bulb, neocortex, hippocampus, anterior colliculus, substantia nigra, the pontine nuclei, inferior olivary nucleus, some nuclei of the cerebral trunk associated with the encephalic nerves, cerebellum, and spinal cord (Katsuyama and Terashima, 2009; Cendelin, 2014).

The Reeler mouse cerebellum is profoundly hypoplastic and, at its surface, only shows very shallow notches, probably the remnants of a tentative foliation (Mikoshiba et al., 1980).

A series of severe histological alterations corresponds to these gross anatomy anomalies: the molecular layer (ML) of the cerebellar cortex is irregular in thickness; the Purkinje cell layer is discontinuous with only few scattered Purkinje neurons (PNs) aligned in their normal position between the more superficial ML and the deeper granular layer (GL), which displays a lower cellular density and a variable thickness, while the remaining PNs

ACCEPTED MANUSCRIPT

are ectopically localized mainly in a central cellular mass intermingled with the white matter (Mariani et al., 1977; Heckroth et al., 1989; Yuasa et al., 1993). Of these alterations, particularly the reduction in GL largely contributes to the atrophy that is macroscopically observed in the Reeler mice (D'Arcangelo and Curran, 1998).

The notion that a form of programmed cell death (PCD) affects the neurons and glia during normal nervous system development, plasticity, and aging, but also in neurodegenerative diseases, is now fully accepted (for a very recent review see Lossi et al., 2015). From the initial observations, several forms of PCD have been described after ultrastructural examination. Schweichel and Merker (1973) were the first to propose a classification of PCD into three types on the basis of role of lysosomes in cell disruption. The first type was originally referred to as heterophagocytosis and mainly corresponds to apoptosis in subsequent classifications (Clarke, 1990). In this case cell death results from phagocytosis and activation of tissue macrophages, without activation of endogenous cell lysosomes. In the second type, sharing several features with necrosis (Clarke, 1990), cell death is induced by an external insult without an obvious lysosome intervention. In the third type, autophagocytosis, cells are eliminated through the activation of their own lysosomal enzymes. This third mode of cell death according to Schweichel and Merker (1973) corresponds to the later described (macro)autophagy (Maiuri et al., 2007).

Among the three forms of PCD, apoptosis has been widely described to massively affect the cerebellar granule cells (CGCs) in the course of their postnatal maturation and migration in several altricial species, including humans (Marzban et al., 2015). Nonetheless, occasional dying neurons displaying the characteristic ultrastructural features of autophagy were also previously observed, albeit occasionally (Lossi and Merighi, 2003).

Although evidence supports the hypothesis that an absence of Reelin causes a loss of the CGCs and the PNs in the cerebellar cortex (Cendelin, 2014), very limited information is available on the occurrence and type of postnatal cell death in mutants. Our group has demonstrated that the CGCs of the Reeler mouse undergo apoptosis after TUNEL labeling of fragmented DNA, and that apoptosis in mutants is significantly higher than in normal wild-type (WT) littermates (Cocito et al., 2016). However, the existence of other death modalities was not investigated, and ultrastructural confirmation is required to assess the

ACCEPTED MANUSCRIPT

type of cell death beyond any reasonable doubt, as DNA fragmentation may also occur in death types other than apoptosis (Lossi et al., 2015).

Therefore, we have expanded our light microscopic investigations on cell death and neurodegeneration during the course of the postnatal cerebellar development of the Reeler mouse, and provided here the first comprehensive ultrastructural description of the modes of death affecting the cerebellar neurons in this mutant. For simplicity, in comparing data between mutants and their WT littermates, we will refer to cell death/neurodegeneration as to different forms of PCD. One should however have well in mind that PCD in WT mice is bona fide naturally occurring neuronal cell death (NOND), whereas in Reeler it is complicated by the effects of the mutation.

2. Materials and Methods

2.1 Animals

Studies were performed on sixteen mice, ranging in age from birth (P0) to postnatal day 15 (P15). Reeler and littermate WT mice at P0, P5, P10 and P15 were used for qualitative and quantitative analysis (n = 4/each postnatal age). The number of animals was kept to a minimum and all efforts were made to minimize their suffering. All experiments were authorized by the Italian Ministry of Health and the Bioethics Committee of the University of Turin. Animal procedures were carried out according to the guidelines and recommendations of the European Union (Directive 2010/63/UE) as implemented by current Italian regulations on animal welfare (DL n. 26-04/03/2014). Before being used in this study, all mice were genotyped to ascertain their appropriate genetic background (D'Arcangelo et al., 1996).

2.2 Histology and ultrastructural analysis

Animals were euthanized intraperitoneally with an overdose of sodium pentobarbital and then perfused with 2% glutaraldehyde+1% paraformaldehyde in Sörensen buffer 0.1 M pH 7.4. Dissected cerebella were then cut in 200 µm thick parasagittal vibratome slices and sections of the vermis were processed according to standard TEM procedures.

For quantitative analysis, a single ultrathin parasagittal section of the entire vermis was collected onto a 75-mesh grid. Due to the small cerebellar size, the area of the grid was

ACCEPTED MANUSCRIPT

sufficient to host the entire section obtained from both WT and Reeler mice at all ages examined. Two different ultrathin sections from the same animal, collected at a distance of at least 200 µm along the transverse plane were subject to analysis. Cells were individually scanned at a magnification ranging between 4,000 to 10,000 X and classified on the basis of their ultrastructure as described in the Results section.

Quantitative results were expressed as the numerical density of cells undergoing PCD per area unit (number of cells undergoing PCD/mm^2). Numerical density was calculated as the ratio of the total number of cells undergoing PCD versus the total number of meshes occupied by tissue. The values so obtained were normalized to area unit by dividing them for the total area of one mesh (0.812 mm^2).

2.3 Statistics

Cell counts obtained from each section pair from the same mouse were subjected to statistical analysis. There were no statistically significant differences in measurements taken from sections belonging to the same animal, thus values were averaged and their means used for analysis. A Student's t-test was used to compare the means obtained for each animal of the same group and between groups. Data were expressed as the mean of the number of cells undergoing to apoptosis or autophagy/mm^2±SEM. Results were considered statistically significant at $p \leq 0.05$.

3. Results

Table 1 summarizes the key ultrastructural features that were used in this study to differentiate between cells undergoing apoptosis or autophagy. A third category of "non-canonical" or dark degenerating cells was also defined. Cells falling into this category: i. did not display the typical characteristics of apoptosis or autophagy, but rather showed a mixture of the features of the two. In some instances some traits typical of necrotic degeneration were also observed; or ii. presented an ultrastructural pattern similar to the so called dark degeneration that was previously described to affect the neurons and glia in the weaver mutant mouse (Migheli et al., 1997), and, more recently, in a murine model of neurodegeneration (Yang et al., 2008). Notably we never found cells with the typical ultrastructural features of pure necrosis.

3.1 NOND in the WT mouse cerebellum

ACCEPTED MANUSCRIPT

3.1.1. Apoptosis

As mentioned in Introduction, apoptosis has been widely documented during the course of postnatal cerebellar NOND in mouse and several other species (Marzban et al., 2015).

Cells with clear characteristics of apoptosis (see Table 1) were observed throughout the entire thickness of the cerebellar cortex (Fig. 1). In keeping with previous observations (Marzban et al., 2015), the CGCs at different stages of differentiation and migration were the main neuronal type affected by apoptosis. Fig. 1 exhibits the ultrastructural features of the apoptotic CGCs at early, intermediate or late stages of the death process. Apoptotic CGCs were visible in both the external granular layer (EGL) and the internal granular layer (IGL) of the forming cerebellar cortex at P0-P15. In the EGL, CGCs undergoing NOND were mainly seen in the more superficial pre-migratory area (Fig. 1A-D). In older age groups, with the progressive disappearance of the EGL as a consequence of the exhaustion of its proliferative capacity and migration of the CGC precursors, apoptotic CGCs were almost exclusively located in the IGL (Fig. 1E-F).

Rare elements of smaller size than the CGCs, with a watery cytoplasm and a more irregular circular contour, could be tentatively identified as glial cells (not shown).

3.1.2. Autophagy

Fig. 2 documents the occurrence of autophagy during postnatal cerebellar development in normal mice. Cells with clear autophagic ultrastructural features (see Table 1) were detected throughout the thickness of the cerebellar cortex. Although occasional inhibitory interneurons displayed an autophagic morphology (Fig. 2A), most autophagic cells were CGCs. As for apoptotic CGCs, autophagic CGCs were detected in both the EGL and IGL (Fig. 2B). Autophagic cerebellar neurons typically had an intact nucleus and a series of cytoplasmic alterations as well as abundance of primary lysosomes with a regularly circular outline, containing a relatively homogeneous electron-dense material. Secondary lysosomes (autophagosomes) of different size and shape and coarsely inhomogeneous contents were also very commonly observed. Vacuoles and phagophores (Fig. 2A-C) were often visible. Rare dystrophic neurites were characterized by the presence of numerous primary and secondary lysosomes of larger dimensions with a very electron-dense uneven content and numerous vacuoles (Fig. 2D).

ACCEPTED MANUSCRIPT

3.2 Cell death and neurodegeneration in the Reeler mouse cerebellum

3.2.1. Apoptosis

Neurons in early (Fig. 3A-B, D, 4B) and late (Fig. 3C, 4A, C) apoptotic phases were observed throughout the thickness of the cerebellar cortex, in the white matter and in the central undifferentiated cellular mass that is typically present in the depth of the Reeler cerebellum. Similarly to WT, apoptosis in the Reeler mouse affects the CGCs during the course of their generation and migration from the EGL to the IGL (Fig. 3, 4B), but also the PNs (Fig. 4A), and the basket cells (Fig. 4C). Rare apoptotic elements were detected in the ML (Figs. 3D, 4C).

3.2.2. Autophagy

Fig. 5 documents the occurrence of autophagy during postnatal cerebellar development in Reeler mice. Neurons that met the criteria for autophagy (see Table 1) have been spotted throughout the thickness of the cerebellar cortex. Autophagic cell changes occurred in the cytoplasm with marked vacuolization (Fig. 5A) and accumulation of primary lysosomes, regular in form and with a relatively homogeneous electron-dense content, and secondary lysosomes, with an uneven electron-dense content and heterogeneous size and shape (Fig. 5A-C). Although CGCs, easily recognizable for their small size, very regular shape and position (Fig. 5A, C), were often observed to display some of the ultrastructural features of autophagy described above, the PNs were the most common cortical neuronal type showing in their cytoplasm all the membranous structures observable along the autophagic process, from the phagophore to the secondary lysosome (Fig. 5B). Autophagic PNs were detected either in the rudimental piriform layer either in the central undifferentiated mass typical of the mutant cerebella.

Quite often, dystrophic neurites were also observed to contain accumulations of very electron-dense primary lysosomes, autophagosomes, and very electron-dense inclusions with an ultrastructure very similar to lipofuscin pigment (Fig. 5D, 6). Very likely most of these neurites belonged to PNs.

3.3 Non canonical death and dark degeneration

ACCEPTED MANUSCRIPT

It was not uncommon to find some neurons with mixed features of apoptosis and autophagy in both WT and Reeler mice, or cells with ultrastructural features not easily fitting into the canonical descriptions of bona fide apoptosis or autophagy (Fig. 7). The latter cells were, at the same time, characterized by nuclear alterations, with chromatin condensation and, at times, pyknosis (Fig. 7A-C), and by profound modifications in the cytoplasm, such as vacuolization (Fig. 7A), general depletion of organelles, presence of primary and/or secondary lysosomes (Fig. 7B), and cell condensation and separation from the surrounding tissue (Fig. 7C). These cells were present in all layers of the cerebellar cortex. They were mostly CGCs (Fig. 7A-B) and, only occasionally, basket cells (Fig. 7C).

In both WT and Reeler mice it was not rare to observe the presence of wide clear electron lucent spaces limited by membranes and surrounded by a normal neuropil (Fig. 4C, 7A). As the surrounding tissue is well preserved, these spaces likely corresponded to the remnants of the neurons undergoing NOND or a mutation-related degenerative process. Very often these cell ghosts contained still well-recognizable membranes of various morphology, some vesicles or, even, the cell nucleus (Fig. 7D).

Finally, both genotypes displayed cells with an uncommonly dark cytoplasm, in the absence of obvious ultrastructural signs of degeneration (Fig. 8A) or in the presence of a certain degree of cell shrinkage with membrane-dense mitochondria and a very irregular nuclear profile (Fig. 8B-C). The latter cells did not show obvious signs of nuclear sufferance.

3.4 Quantitative analysis

The density (number of cells /mm^2) of neurons displaying apoptotic or autophagic features was calculated irrespectively of type (i.e. CGCs, PNs, basket and Golgi cells) and independently of cell position in the different layers of the cerebellar cortex (Table 3). Notably, the density of apoptotic neurons, irrespective of the genotype and age, was constantly higher than that of autophagic neurons.

In WT mice the density of apoptotic neurons progressively decreased from birth to P15 with a statistically significant drop from P10 onward (Student's t test: P0/P10 p= 0.041; P0/P15 p= 0.021) whereas reduction in the density of apoptotic neurons was not statistically significant across five-day intervals. These data demonstrate that, in normal

ACCEPTED MANUSCRIPT

mice, apoptotic NOND is a quite regular process during the two first postnatal weeks of cerebellar development. The trend was the opposite in Reeler where the density of apoptotic neurons increased from birth to P15 but with an oscillatory irregular trend (Student's t test: P0/P5, P0/P10 and P0/P15 not significant; P5/P10 $p = 0.008$; P5/P15 $p = 0.038$; P10/P15 $p = 0.008$). When animals of corresponding ages and different genotypes were compared, there was a statistically significant difference at P15 (Student's t test: WT 11.01±.1.69, Reeler 44.29±7.64; $p = 0.005$), but not at early developmental stages.

In WT mice the density of autophagic neurons did not display statistically significant differences in the time interval examined in this study. These data demonstrate that, in normal mice, autophagy is a constant process along the two first postnatal weeks of cerebellar development. Similarly to apoptosis, the density of autophagic neurons also raised in Reeler from birth to P15, but with statistically significant differences only from P5 onward (Student's t test: P5/P15 $p= 0.039$; P10/P15 $p= 0.008$). When animals of corresponding ages and different genotypes were compared, there was a statistically significant difference at P10 (Student's t test: P10 WT 5.24±0.88, Reeler 0.79±0.50 $p= 0.005$). Notably, the density of autophagic neurons was reduced in Reeler in the P0-P10 interval, but increased at P15.

4. Discussion

PCD is a widespread phenomenon during the course of animal development. Since its initial recognition in the form of apoptosis (to the point that the two terms are still erroneously used as synonyms), several other types of cell death have been described and, today, it is clear that apoptosis is simply one of the several modalities by which the number of cells is regulated during the course of histogenesis and organogenesis.

In the nervous system, the diversity of the ultrastructural morphological patterns of NOND, was initially described by Schweichel and Merker (1973) and, later, by Clarke (1990). In general, these authors recognized three different ultrastructural types of cell death: apoptotic (Type 1), cytoplasmic non-lysosomal, i.e. necrotic (Type 2), and autophagic (Type 3). However, more recent studies have described additional ultrastructural patterns which did not fit the tripartite classification above, as the situation changes dramatically when the nervous system is subjected to any kind of insults, such as genetic mutations, infections or neurodegeneration.

ACCEPTED MANUSCRIPT

Among spontaneous mutations affecting the CNS, those primarily striking the mouse cerebellum have been long ago discovered (Table 2). They attracted the attention of the investigators not only as possible models of human ataxias (Cendelin, 2014), but also as invaluable tools to study the normal cerebellar development in times when genetic engineering was still in its infancy. In the course of the following decades, analysis of these mutants clearly demonstrated the occurrence of an array of cell death typologies, with often mixed features (Table 4). Species-specific responses may be an additional complicating factor in the study of neural death, as well as inter-area anatomical/functional differences. For example, contrasting results were obtained after ischemia or stroke in several mammalian species, as mixed apoptotic/necrotic figures were described in rat (Wei et al., 2006) or mouse (Pamenter et al., 2012), whereas no evidence of apoptosis was described in gerbils (Colbourne et al., 1999), and apoptosis and necrosis occurred in separate neuronal populations in dogs (Martin et al., 2000). Likewise, death in prionic infection was reported to be autophagic by some authors (Liberski et al., 2008) but others denied the occurrence of autophagy and, instead, described a novel, non-apoptotic, non-autophagic form of neuronal death in a transgenic mouse model (Christensen et al., 2010). Finally, a cross-talk between neuronal apoptosis and autophagy was described in a mouse model of Alzheimer's disease, highlighting the concept that such an interaction had important consequences in the ultimate survival of neurons in the course of neurodegeneration (Yang et al., 2008).

Altogether these examples outline the diversity of forms that death assumes in neurons (and glia) under different physiological and pathological conditions. It was therefore not surprising that such diversity was also reflected in the present analysis of cell death in the course of the postnatal cerebellar development of the normal and Reeler mice. It may appear quite bizarre that previous analysis of cell death in classic cerebellar mutant mice, that is Reeler, Lurcher, Purkinje cell degeneration (pcd), nervous, Weaver, and Staggerer mice, was often disjointed by a comparison with their normal counterpart, unless, but at times only, in terms of the quantitation and timing of degenerating neurons (Table 4).

4.1 NOND in cerebellar development

The occurrence of NOND during the course of normal cerebellar development has been widely described in several species including humans (reviewed in Marzban et al., 2015).

ACCEPTED MANUSCRIPT

Historically, death was first documented by merely histological techniques that allowed detecting nuclear fragmentation and pyknosis (see e.g. Lewis, 1975). The availability of more "specific" methods, such as TUNEL for detecting DNA fragmentation (Wood et al., 1993) and activated caspase 3 immunocytochemistry (Lossi et al., 2004), subsequently permitted demonstration that PCD was apoptotic. The temporal window of apoptosis in cerebellum coincides with the first two postnatal weeks in rodents (rat, mouse) and rabbits, and the first postnatal trimester in humans. Nonetheless, comparatively few ultrastructural studies are available to confirm the apoptotic nature of postnatal cerebellar NOND (Lossi et al., 2002; Lossi and Merighi, 2003). In their review, Marzban et al. (2015) have concluded that: the data available so far indicate that (apoptotic) cell death occurs in the developing cerebellum to a limited extent, particularly in the EGZ (here referred to as EGL) among recently post-mitotic cells and to a lesser extent in the granular layer (here referred to as IGL). The reported extent to which this occurs varies widely, but overall it seems reasonable to estimate that a maximum 5% of granule cells and a smaller proportion of Purkinje cells are lost, although it must be noted that studies in the very early developmental stages are lacking. Therefore, detection of apoptotic CGCs in our material was not surprising (see also Lossi and Gambino, 2008). It was instead totally surprising to obtain ultrastructural evidence of autophagy in CGCs and PNs. In WT mice the density of autophagic neurons did not display statistically significant differences in the time interval examined in this study. Autophagy is a self-degradative lysosomal process used for degrading and recycling various cellular constituents (Klionsky et al., 2012). Studies in murine transgenic models converged to indicate that autophagy is constitutively active during the course of neurodevelopment, being suspected to be the primary cause of non-apoptotic cellular demise, but, at the same time, of neuronal survival (Rami, 2009). As to the possibility that autophagy is protective to neurons, studies in vitro on isolated neurons and cerebellar slices have shown, for example, that the autophagy-related Unc51.1 murine gene signals the program of gene expression leading to the formation of the CGC axons (Tomoda et al., 1999). In addition, the selective ablation of two other autophagy-related genes (Atg5 or Atg7) leads to behavioral deficits associated with severe neuronal loss in the cerebellar cortex, and dystrophy of PN axon terminals in the deep cerebellar nuclei (Komatsu et al., 2006; Komatsu et al., 2007a; Komatsu et al., 2007b). On the other hand, in contrast to neuroprotection, neuronal cell death may also involve autophagy: autophagy precedes and is causally connected with the subsequent onset of

ACCEPTED MANUSCRIPT

CGC apoptosis in vitro (Canu et al., 2005), and dysfunction of endosomal sorting complex required for transport 3 (ESCRT-3) causes autophagosome accumulation and neurodegeneration of PNs (Lee et al., 2007). Therefore, whereas it remains to be fully clarified whether autophagy is the firefighter and/or the pyromaniac in NOND (Rami, 2009), our present data provide an unequivocal proof of the occurrence of autophagy of CGCs and PNs during the course of normal cerebellar development. Reduction in the density of autophagic neurons in Reeler in the P0-P10 interval, but its increase at P15 is difficult to be explained without further functional studies. On a purely speculative basis it seems possible that autophagy exerts a protective role against apoptotic PCD in WT animals, as this might explain the abrupt rise in the density of apoptotic cells at P15 in the Reeler only.

In this study we have also observed a limited number of neurons displaying a mix of the ultrastructural features typical of the single forms of PCD. In particular the occurrence of cells with concurrent apoptotic/autophagic morphologies is in line with the aforementioned cross-talk between apoptosis and autophagy that was described in a mouse model of Alzheimer disease (Yang et al., 2008) and highlights that such a cross-talk very likely also occurs in the course of NOND and is exacerbated in the Reeler phenotype. In keeping with this possibility, we have previously shown that, in organotypically cultured cerebellar slices, the main anti-apoptotic protein B-cell lymphoma 2 (Bcl-2) is post-translationally regulated in CGCs in parallel with the expression of beclin-1, a protein that participates in the regulation of autophagy (Lossi et al., 2010).

4.2 Cell death in spontaneous cerebellar mutants: what can we learn about normal cerebellar development?

4.2.1 Cell death and neurodegeneration in Reeler

The Reeler mutation has been extensively studied, and, among the numerous structural changes in the cerebellar cortex architecture, a significant reduction in the number of PNs and density of CGCs was reported (references in Table 2), in parallel with the misplacement of these neurons in various locations within the cerebellar cortex and in the depth of the cerebellar white matter. That the mechanisms of cell death in Reeler have been poorly investigated is not surprising: as the mutation primarily affects neuronal migration (D'Arcangelo et al., 1995), the reduction in the numbers of CGCs and PNs has

ACCEPTED MANUSCRIPT

always been interpreted as a consequence of the cytoarchitectonic disorganization, and, has thus received comparatively little attention. Therefore, there was a complete lack of information about the ultrastructural features of degenerating neurons in the mutant.

Although the adult Reeler mice were described to have lower neurogenesis rates in the forebrain (Won et al., 2006), we have been unable to find statistically significant differences in the rate of cell proliferation between mutants and WT mice during postnatal cerebellar neurogenesis, but rather observed increased apoptosis in Reeler from P15 onward (Cocito et al., 2016). The quantitative ultrastructural data reported here, albeit limited to the cerebellar vermis, are fully in line with these light microscopy observations, where the entire cerebellum was subjected to analysis. As Cocito et al. (2016) ascertained cell death with TUNEL, the contribution of autophagy was not evaluated, nor could the type(s) of cells undergoing PCD be determined in full, with the exception of the CGCs. Therefore, the present analysis adds further information related to the type of PCD (apoptosis and autophagy) and the affected cells (CGCs and PNs).

Manuscript

4.2.2. Comparative analysis of cell death/neurodegeneration in cerebellar mutants

For the sake of brevity, in Tables 2 and 4 we have summarized the main features of the cerebellar phenotype, with particular reference to cell death, in Reeler, Lurcher, Purkinje cell degeneration (pcd), nervous, Weaver, and Staggerer mice.
A common thread links these mutants, as neurodegeneration/death mainly affects the PNs and the CGCs. However, the type of death striking these two types of neurons is often controversial, particularly regarding PNs in Lurcher (Table 4). Altogether the pattern of neuronal degeneration in Lurcher indicates that multiple PN death pathways are induced as a consequence of the mutation. Similarly, our present observations suggest that the cells displaying "non-canonical" mixed forms of death in Reeler are likely the results of a mixed activation of several PCD mechanisms. Notably, these forms have been also observed in WT mice, confirming, as discussed above, that the interplay of apoptosis and autophagy may be more common than previously expected.

A point of difference among mutants other than Reeler is instead that, with the exception of Weaver, where the apoptotic death of CGCs is a primary consequence of the mutation (Goldowitz and Mullen, 1982), CGC die secondary to the degeneration of PNs in all the

ACCEPTED MANUSCRIPT

others (Table 4). In the Staggerer, for example, using Staggerer-wild type chimeras, it was suggested that PN alterations defects are cell-intrinsic (Herrup and Mullen, 1979b; Herrup and Mullen, 1981), whereas the Staggerer CGCs are rescued in the chimeras, demonstrating that death of these neurons is indirectly linked to mutation (Herrup and Sunter, 1987). Also, studies on chimeric mice revealed that degeneration affects Weaver PNs but not non-Weaver PNs, indicating that, while the disorganization of PNs is an indirect effect, their degeneration is a direct result of the DNA alteration (Smeyne and Goldowitz, 1990).

In general and comparative terms, it is not surprising that cell death in mutants was observed to effect mainly the CGCs and the PNs, as these are the two most abundant types of cerebellar cortical neurons and their synaptic interactions are reciprocally important in survival regulation (Altman, 1992). Notably, the lower density of CGCs in Reeler accompanies the drastic reduction of synaptic contacts between the PNs and the parallel fibers (Mariani et al., 1977; Castagna et al., 2014). It is also remarkable that we have previously shown the occurrence of target-dependent (in the IGL) and target-independent (in the EGL) apoptosis during the course of normal cerebellar development in rabbit (Lossi et al., 2002). It is therefore not surprising that in the extensively investigated Lurcher mouse, where CGC neurodegeneration is secondary to PN death and hence related to the proper formation of synapses with target, the death of CGCs only takes the form of a bona fide apoptosis.

This study also shows that autophagy occurs in Reeler CGCs. As mentioned in 4.1, it remains unclear whether or not autophagy plays a pro- or an anti-survival role in the course of cerebellar development. It is worth noting that down-regulation of the Apaf1 gene, which is involved in the formation of apoptosome, results in activation of an autophagy program in the cerebral cortex (Moreno et al., 2006). Therefore it is reasonable, also considering the temporal analysis of apoptotic/autophagic cell densities in our material, that autophagy may be protective to the CGCs, as its reduction in the P10 Reeler cerebellum opens the way for the subsequent increase in apoptosis that we observed at P15.

5. Conclusion

ACCEPTED MANUSCRIPT

More and more data have been added to support the notion of an interplay between apoptosis and autophagy, not only when the cell microenvironment is experimentally manipulated in vitro (Moreno et al., 2006), but also when neurodegeneration occurs in vivo as exemplified in certain conditions such as Alzheimer's disease (Yang et al., 2008; Nixon, 2013). Under this perspective, the study of Lurcher and Reeler, in which a multiplicity of death pathways has unequivocally been demonstrated, but in which it is likely that evidence will also be found of the other classical mutants, where the current picture is fuzzier, will surely continue to be informative about the mechanisms of normal cerebellar development and their alterations under diseased conditions.

Accepted Manuscript

ACCEPTED MANUSCRIPT

Apoptosis	Autophagy	Dark degeneration
Nuclear changes Initial chromatin condensation and segregation into sharply delineated electron-dense granular masses that abut the nuclear envelope. Pyknosis. Disorganization of nucleolus Overall shape becomes irregular Fragmentation into membrane-bounded apoptotic bodies Nuclear envelope intact until very late stages **Cytoplasmic changes** Condensation Appearance of few vacuoles Overall cell shape may become irregular Packaging of intact organelles as a consequence of significant cytosolic loss Detachment of ribosomes from RER Presence of numerous polysomes that eventually disappear Intact organelles	**Nuclear changes** Absent **Cytoplasmic changes** Abundance of vacuoles Phagophores and/or autophagosomes engulfed with cytoplasmic components Primary lysosomes Secondary autophagolysosomes Dystrophic swollen neurites filled with vacuoles, autophagosomes, secondary autophagolysosomes	**Nuclear changes** General increase in electrondensity in the absence of chromatin condensation or other alterations typical of apoptosis **Cytoplasmic changes** Strong increase in electrondensity Vacuolization of variable severity with variable degree of organelles' dilatation Absence of typical autophagic changes Accumulation of lipofuscin granules

Table 1: Ultrastructural criteria for classification of cell death

Accepted Manuscript

ACCEPTED MANUSCRIPT

Mutants	Mutated gene/Encoded protein	Dominance	Genotype of affected animals	Phenotype	References
Reeler	Reln/Reelin	NO	$Reln^{-/-}$	Cerebellar atrophy/hypoplasia Disorganization of cortical architecture Reduction in number of PNs Reduction in density of CGCs	Falconer, 1951; Mariani et al., 1977; Mikoshiba et al., 1980; Heckroth et al., 1989; Yuasa et al., 1993; D'Arcangelo et al., 1995; Katsuyama and Terashima, 2009
Lurcher	$Grid2^{Lc}$/GluRδ2	Partial	$Lc^{+/+}$	Lethal (inability to feed with milk)	Phillips, 1960; Cheng and Heintz, 1997; Zuo et al., 1997
			$Lc^{+/-}$	Postnatal degeneration of PNs, CGCs, stellate and basket cells and inferior olive neurons	
Pcd	$Agtpbp1^{pcd/J}$/ AGTPBP1	NO	$Pcd^{-/-}$	Postnatal loss of virtually all PNs, slow, progressive degeneration of the retina and olfactory bulb mitral cells	Fernandez-Gonzalez et al., 2002
Nervous	Nr*	NO	$Nr^{-/-}$	Degeneration of PNs	Campbell and Hess, 1996
Staggerer	$Rora^{sg}$/Rora	NO	$Sg^{-/-}$	Alteration of PN alignment Degeneration of PNs Reduction in number of CGCs	Sidman et al., 1962; Hamilton et al., 1996
Weaver	$Kcnj6^{Wv}$/GIRK2	Partial	$Wv^{+/-}$	Cerebellar atrophy/hypoplasia Alterations more prominent in vermis Mild loss of PNs Misalignment of PNs Disorganization/ reduction of EGL Degeneration of CCGs and loss of contact with the Bergmann glia	Rakic and Sidman, 1973; Smeyne and Goldowitz, 1989; Patil et al., 1995
			$Wv^{+/+}$	Exacerbation of the $Wv^{+/-}$ phenotype with total loss of EGL and widespread degeneration of CGCs Death at weaning	

Table 2: Classic cerebellar mutant mice

ACCEPTED MANUSCRIPT

Abbreviations: AGTPBP1 = cytosolic ATP/GTP binding protein 1; CGCs = cerebellar granule cells; EGL = external granular layer of the forming cerebellar cortex; GIRK2 = G protein-coupled inwardly-rectifying potassium channel 2; GluRδ2 = δ2 glutamate receptor; Pcd = Purkinje cell degeneration; PNs = Purkinje neurons; Rora = retinoid-related orphan receptor alpha; *not yet cloned – mechanism of action unknown.

Accepted Manuscript

ACCEPTED MANUSCRIPT

Genotype	Age	Apoptotic neurons/ mm^2±SEM	Autophagic neurons/ mm^2±SEM
Wild-type *Reln*$^{+/+}$	P0	47.19±11.57	6.89±1.28
	P5	27.83±7.12	10.49±4.37
	P10	16.22±2.82	5.24±0.88
	P15	11.01±.1.69	4.36±2.39
Reeler *Reln*$^{-/-}$	P0	28.57±4.31	4.63±1.57
	P5	32.94±1.12	1.83±1.25
	P10	23.08±2.27	0.79±0.50
	P15	44.29±7.64	6.92±1.48

Table 3: Quantitation of apoptotic and autophagic neurons in cerebellar vermis of postnatal wild-type and Reeler mice

Accepted Manuscript

ACCEPTED MANUSCRIPT

Mutants	Type(s) of dying neurons	Type(s) of death	Temporal window/% of death	References
Reeler	PNs	Apoptotic Autophagic Dark degeneration	P0-P15*	Cocito et al., 2016 This study
	CGCs			
	Basket and Golgi cells	Dark degeneration		
Lurcher	PNs	Exocytotic apoptosis	P8-P65/progressive total loss	Caddy and Biscoe, 1979; Zuo et al., 1997
		Necrotic		Dusart et al., 2006
		Autophagic		Yue, 2010; Yue et al., 2002
		Necrotic+Autophagic		Nishiyama and Yuzaki, 2010
	CGCs	Apoptotic	Follows death of PNs/progressive, 90% at P60	Caddy and Biscoe, 1979; Norman et al., 1995
	Basket and stellate cells	N/A		Caddy and Biscoe, 1979
Pcd	PNs	Apoptotic	P20-P28/almost 100%	Chakrabarti et al., 2009
		Autophagic		Berezniuk et al., 2010
	CGCs	N/A	Secondary to PN death	Triarhou, 2010
Nervous	PNs	Necrosis	P9-P50/80-97% depending on lobules	Landis, 1973; Li et al., 2013
Staggerer	PNs	N/A	P30/60-90%regionally variable loss Cell-intrinsic	Herrup and Mullen, 1979a
	CGCs	Apoptotic*	P28/almost 100% Secondary to PN death	Landis and Sidman, 1978; Herrup and Busser, 1995
Weaver	PNs	Non-necrotic** Non-apoptotic**	86% in $Wv^{+/-}$ 72% $Wv^{+/+}$	Blatt and Eisenman, 1985; Herrup and Trenkner, 1987; Migheli et al., 1997
	CGCs	Apoptotic		Migheli et al., 1995; Migheli et al., 1997

Table 4: Types of degenerating cells and death features in classic cerebellar mutant mice

Abbreviations: CGCs = cerebellar granule cells; N/A = data not available; PNs = Purkinje neurons; *but negative TUNEL staining (Herrup and Busser, 1995) ** (Migheli et al., 1997)

Accepted Manuscript

ACCEPTED MANUSCRIPT

Figure legends

Figure 1: Apoptosis in the WT mouse. **A**: A CGC showing early apoptotic features in the deep EGL of a P0 WT mouse. Chromatin is typically set against the inner nuclear envelope in the form of crescent-like accumulations. A nearby CGC shows an intact ultrastructural morphology. **B**: A CGC showing late apoptotic features in the deep EGL of a P0 WT mouse. The nucleus is pyknotic with highly condensed chromatin. The cytoplasm is profoundly altered with accumulation of electron-dense coarsely granular material and several vesicles. A nearby CGC shows an intact ultrastructural morphology. **C**: Low magnification view of the EGL in a P10 WT mouse. A CGC with typical apoptotic ultrastructure displays a very electron-dense partly condensed nucleus. A mitotic cell can be partially seen on the bottom left corner of image. The asterisk indicates a blood capillary at the pial surface of the cerebellar cortex. The area indicated in the rectangle is enlarged in D. **D**: High magnification view of the apoptotic CGC in C. Two very dense apoptotic bodies (ab) are clearly visible. The cytoplasm displays an initial retraction and a large vacuole (asterisks) **E**: A CGC showing late apoptotic features in the IGL of a P15 WT mouse. Note the intense condensation of the nucleus and overall cell shrinkage. The cell is shown at higher magnification in F. **F**: High magnification view of the apoptotic CGC in E. Note the higher degree of cytoplasm condensation compared to the apoptotic CGC in D. Abbreviations: ab = apoptotic body, CGC = cerebellar granule cell; EGL = external granular layer; IGL = internal granular layer; m = mitosis; nu = nucleus; P = postnatal day. Bars = 1 μm.

Figure 2: Autophagy in the WT mouse. **A**: A Golgi cell (Go) at the IGL surface of a P5 mouse displays an ultrastructurally normal nucleus while the cytoplasm is full of vacuoles and primary/secondary lysosomes with uneven dimensions and a strongly electron-dense content. The arrowheads indicate a phagophore which is winding a portion of cytoplasm to form a phagosome. **B**: A CGC in the IGL of a P10 mouse with autophagic ultrastructural features. The nucleus is normal and the cytoplasm contains numerous vacuoles and primary lysosomes. A large secondary lysosome (arrow) displays a strongly electron-dense content, with inhomogeneous granular material and vesicles. **C**: High magnification view of an autophagosome in the IGL of a P5 WT mouse. Note the double-layer membranes surrounding a partially degraded mitochondrion (asterisk). **D**: A dystrophic neurite in IGL of a P5 WT mouse with typical autophagic features (several primary lysosomes, a large dark secondary lysosome marked by an arrow, and a few vesicles. Abbreviations: EGL = external granular layer; Go = Golgi cell; IGL = internal granular layer; nu = nucleus; PN = Purkinje neuron; P = postnatal day. Bars = 1 μm

Figure 3: Apoptosis in the P0 Reeler mouse. **A**: Low magnification view showing the ultrastructure of the deep portion of the cerebellar cortex (IGL/central mass). The disorganization of the layered cerebellar structure is clearly evident: cortical neurons are mixed in apparent disorder and separated by neuropil which is being organized. The clear, larger cells are PNs, while the dark, smaller cells are CGCs. Two apoptotic CGCs are clearly recognizable (arrows) for the strongly electron-dense nucleus with condensed chromatin.

ACCEPTED MANUSCRIPT

The area in the rectangle is shown at higher magnification in B. **B**: High magnification detail of panel A showing a CGC in mid-to-late phase of apoptosis. **C**: Apoptotic bodies (ab) at the outer border of IGL. **D**: Apoptotic migrating CGC in the ML. The nucleus is strongly electron-dense but not pyknotic yet, with a coarsely granular appearance and scattered fragments of nuclear envelope. Cytoplasm organelles are almost absent. The cell is surrounded by tightly packed parallel fibers. ab = apoptotic body; CGC = cerebellar granule cell; IGL = internal granular layer; ML = molecular layer; nu = nucleus; P = postnatal day; PN: Purkinje neuron. Bars = 1 μm

Figure 4: Apoptosis in the Reeler mouse. **A**: Apoptotic PN in the IGL/central mass at P0. The cell nucleus is pyknotic and partly fragmented with vesicles of different size and appearance. The clear cytoplasm appears largely empty with only rare membranes of the endoplasmic reticulum and ribosomes. An ultrastructurally normal PN and a CGC can be appreciated at left and right, respectively. The asterisk indicates the lumen of a blood vessel **B**: Apoptotic CGC in the IGL of a P5 Reeler mouse (bottom left). Condensed chromosomes can be easily seen in a large mitotic cell (top right). **C**: Apoptotic basket cell (recognized by its location, size, and horizontal orientation) in the ML at P15. The cell has a very dark highly condensed electron-dense nucleus and uneven, scant cytoplasm poor in organelles. At the top, close to the surface of the cortex (asterisk) some electron lucent areas are visible (arrowheads) likely corresponding to the spaces left empty by the dissolution of cells undergoing PCD. Abbreviations: CGC = cerebellar granule cell; IGL = internal granular layer; m = mitosis; ML = molecular layer; nu = nucleus; P = postnatal day; PN: Purkinje neuron. Bars = 500 nm

Figure 5: Autophagy in the Reeler mouse. **A**: CGC with ultrastructural characters of autophagy in the deep IGL at P0. The cell presents an intact nucleus while in the cytoplasm is markedly vacuolated with primary and secondary lysosomes of inhomogeneous content. **B**: Purkinje neuron with characters of autophagy in the IGL/central mass at P5. Very electron-dense primary and secondary lysosomes are present in the cytoplasm (enlarged in the box on the bottom right), indicative of autophagic activity. The nucleus is intact with unaffected nucleoplasm. **C**: CGC with characters of autophagy in the IGL at P15. The cell nucleus is normal while the cytoplasm is packed with vesicles and primary and secondary lysosomes. **D**: A large dystrophic neurite with autophagic features in the IGL at P15. The neurite is full of electron-dense vesicles of inhomogeneous size some of which are clearly identifiable as primary lysosomes. CGC = cerebellar granule cell; IGL = internal granular layer; P = postnatal day; PN: Purkinje neuron. Bars = 1 μm

Figure 6: Dystrophic neurites in the Reeler mouse. **A**: Dystrophic neurites with autophagic features in IGL at P0. Neurites contain numerous electron-dense granules of variable size and uneven appearance. **B**: Dystrophic neuritis with autophagic features in IGL at P0. A large secondary lysosome can be easily appreciated (arrow). **C**: Large dystrophic neurite (arrows) in the ML at P15. An apoptotic CGC is also visible, separated by surrounding tissue by an electron lucent halo as a consequence of cell shrinkage.

ACCEPTED MANUSCRIPT

Abbreviations: CGC = cerebellar granule cell; IGL = internal granular layer; ML = molecular layer; P = postnatal day. Bars = 1 µm

Figure 7: Atypical forms of PCD in postnatal cerebellum. **A**: A presumptive CGC in the IGL of the P0 Reeler mouse. The nucleus is pyknotic with typical apoptotic features, whereas the cytoplasm displays numerous vacuoles and electron-dense bodies typical of autophagy. **B**: CGC at the border between the ML and IGL in P5 Reeler mouse. The electron-dense nucleus displays chromatin condensation, and the cytoplasm appears free from organelles with rare vesicles, one of which is very electron-dense and likely corresponds to a large primary lysosome. **C**: A degenerating basket cell at P10, located deeply in the ML (asterisk) has its major axis typically orientated parallel to the surface of the cerebellar lamina. An ultrastructurally healthy basket cell is visible in the upper half of the image. **D**: Wide electron lucent spaces (asterisks) corresponding to cellular ghosts in the IGL of a P15 WT mouse. The upper space likely corresponds to the degenerated cytoplasm of a CGC with an intact nucleus (arrows) and little preserved cytoplasm. Abbreviations: EGL = external granular layer; Ba = basket cell; IGL = internal granular layer; ML = molecular layer; nu = nucleus; P = postnatal day. Bars = 1 µm

Figure 8: Dark neuronal degeneration in postnatal cerebellum. **A**: Initial phase of dark neuronal degeneration in the piriform layer of a P10 WT mouse. The degenerating PN is more electron-dense compared to the surrounding cells, one of which is partly shown in the lower left corner of the image. Notably, the cell maintains a normal appearance of both its nucleus and cytoplasm, where cell organelles with normal morphology and distribution can be appreciated. **B**: Late phase of dark neuronal degeneration in a PN of a P15 WT mouse. The nuclear profile is very irregular; the nucleoplasm is homogeneous without obvious heterochromatin. The cytoplasm is very dense with many organelles tightly packed and displaying an anomalous accumulation of intensely stained membranes of the endoplasmic reticulum. Nearby intact CGCs are visible at the top right corner of the image. **C**: Late phase of dark degeneration in two PNs of a P15 Reeler mouse. The two neurons have ultrastructural features remarkably similar to those showed in B. The irregular layering of the cortex in the central mass, typical of the mutant, is clearly seen. Abbreviations: CGC = cerebellar granule cell; IGL = internal granular layer; P = postnatal day; PN = Purkinje neuron. Bars = 500 nm

Accepted Manuscript

ACCEPTED MANUSCRIPT

References

Altman, J. 1992. Programmed cell death: the paths to suicide. Trends Neurol. Sci. 15, 278-280.

Berezniuk, I., J. Sironi, M. B. Callaway, L. M. Castro, I. Y. Hirata, E. S. Ferro, L. D. Fricker. 2010. CCP1/Nna1 functions in protein turnover in mouse brain: Implications for cell death in Purkinje cell degeneration mice. FASEB J. 24, 1813-1823.

Blatt, G. J. and L. M. Eisenman. 1985. A qualitative and quantitative light microscopic study of the inferior olivary complex of normal, reeler, and weaver mutant mice. J. Comp. Neurol. 232, 117-128.

Caddy, K. W. and T. J. Biscoe. 1979. Structural and quantitative studies on the normal C3H and Lurcher mutant mouse. Philos. Trans. R. Soc. Lond. B. 287, 167-201.

Campbell, D. B. and E. J. Hess. 1996. Chromosomal localization of the neurological mouse mutations tottering (tg), Purkinje cell degeneration (pcd), and nervous (nr). Mol. Brain Res. 37, 79-84.

Canu, N., R. Tufi, A. L. Serafino, G. Amadoro, M. T. Ciotti, P. Calissano. 2005. Role of the autophagic-lysosomal system on low potassium-induced apoptosis in cultured cerebellar granule cells. J. Neurochem. 92, 1228-1242.

Castagna, C., P. Aimar, S. Alasia, L. Lossi. 2014. Post-natal development of the Reeler mouse cerebellum: An ultrastructural study. Ann. Anat 196, 224-235.

Cendelin, J. 2014. From mice to men: lessons from mutant ataxic mice. Cerebellum & Ataxias 1, 4.

Chakrabarti, L., J. Eng, N. Ivanov, G. A. Garden, A. R. La Spada. 2009. Autophagy activation and enhanced mitophagy characterize the Purkinje cells of pcd mice prior to neuronal death. Molecular Brain 2, 24.

Cheng, S. S. and N. Heintz. 1997. Massive loss of mid- and hindbrain neurons during embryonic development of homozygous lurcher mice. J Neurosci. 17, 2400-2407.

Christensen, H. M., K. Dikranian, A. Li, K. C. Baysac, K. C. Walls, J. W. Olney, K. A. Roth, D. A. Harris. 2010. A Highly Toxic Cellular Prion Protein Induces a Novel, Nonapoptotic Form of Neuronal Death. Am.J.Pathol.176, 2695-2706.

Clarke, P. G. H. 1990. Developmental cell death: morphological diversity and multiple mechanisms. Anat. Embryol. 181, 195-213.

Cocito, C., L. Lossi, A. Merighi. 2016. A neurochemical study of the postnatal Reeler cerebellum. Front. Cell Neurosci. *in preparation*

Colbourne, F., G. R. Sutherland, R. N. Auer. 1999. Electron Microscopic Evidence against Apoptosis as the Mechanism of Neuronal Death in Global Ischemia. J. Neurosci. 19, 4200-4210.

D'Arcangelo, G. and T. Curran. 1998. Reeler: new tales on an old mutant mouse. Bioessays 20, 235-244.

D'Arcangelo, G., G. G. Miao, S. C. Chen, H. D. Soares, J. I. Morgan, T. Curran. 1995. A protein related to extracellular matrix proteins deleted in the mouse mutant reeler. Nature 374, 719-723.

ACCEPTED MANUSCRIPT

D'Arcangelo, G., G. G. Miao, T. Curran. 1996. Detection of the reelin breakpoint in reeler mice. Brain Res. Mol Brain Res. 39, 234-236.

Dusart, I., J. Guenet, C. Sotelo. 2006. Purkinje cell death: Differences between developmental cell death and neurodegenerative death in mutant mice. Cerebellum 5, 163-173.

Falconer, D. S. 1951. Two new mutants, 'trembler' and 'reeler', with neurological actions in the house mouse (*Mus musculus L.*). J. Genet 50, 192-201.

Fernandez-Gonzalez, A., A. R. L. Spada, J. Treadaway, J. C. Higdon, B. S. Harris, R. L. Sidman, J. I. Morgan, J. Zuo. 2002. Purkinje cell degeneration (pcd) Phenotypes Caused by Mutations in the Axotomy-Induced Gene, Nna1. Science 295, 1904-1906.

Goldowitz, D. and R. J. Mullen. 1982. Granule cell as a site of gene action in the weaver mouse cerebellum: evidence from heterozygous mutant chimeras. J. Neurosci. 2, 1474-1485.

Hamilton, B. A., W. N. Frankel, A. W. Kerrebrock, T. L. Hawkins, W. FitzHugh, K. Kusumi, L. B. Russell, K. L. Mueller, V. van Berkel, B. W. Birren, L. Kruglyak, E. S. Lander. 1996. Disruption of the nuclear hormone receptor ROR[alpha] in staggerer mice. Nature 379, 736-739.

Heckroth, J. A., D. Goldowitz, L. M. Eisenman. 1989. Purkinje cell reduction in the reeler mutant mouse: A quantitative immunohistochemical study. J.Comp.Neurol. 279, 546-555.

Herrup, K. and J. C. Busser. 1995. The induction of multiple cell cycle events precedes target-related neuronal death. Development 121, 2385-2395.

Herrup, K. and R. J. Mullen. 1981. Role of the Staggerer gene in determining Purkinje cell number in the cerebellar cortex of mouse chimeras. Brain Res. 227, 475-485.

Herrup, K. and K. Sunter. 1987. Numerical matching during cerebellar development: quantitative analysis of granule cell death in staggerer mouse chimeras. J. Neurosci. 7, 829-836.

Herrup, K. and E. Trenkner. 1987. Regional differences in cytoarchitecture of the weaver cerebellum suggest a new model for weaver gene action. Neuroscience 23, 871-885.

Herrup, K. and R. J. Mullen. 1979a. Regional variation and absence of large neurons in the cerebellum of the staggerer mouse. Brain Res. 172, 1-12.

Herrup, K. and R. J. Mullen. 1979b. Staggerer chimeras: Intrinsic nature of purkinje cell defects and implications for normal cerebellar development. Brain Res. 178, 443-457.

Katsuyama, Y. and T. Terashima. 2009. Developmental anatomy of reeler mutant mouse. Dev., Growth & Differ. 51, 271-286.

Klionsky, D. J., F. C. Abdalla, H. Abeliovich, R. T. Abraham, A. Acevedo-Arozena, K. Adeli, L. Agholme, M. Agnello, P. Agostinis, J. A. Aguirre-Ghiso, H. J. Ahn, O. Ait-Mohamed, S. Ait-Si-Ali, T. Akematsu, S. Akira, H. M. Al-Younes, M. A. Al-Zeer, M. L. Albert, R. L. Albin, J. Alegre-Abarrategui, M. F. Aleo, M. Alirezaei, A. Almasan, M. Almonte-Becerril, A. Amano, R. K. Amaravadi, S. Amarnath, A. O. Amer, N. Andrieu-Abadie, V. Anantharam, D. K. Ann, S. Anoopkumar-Dukie, H. Aoki, N. Apostolova, G. Arancia, J. P. Aris, K. Asanuma, N. Y. Asare, H. Ashida, V. Askanas, D. S. Askew, P. Auberger, M. Baba, S. K. Backues, E. H. Baehrecke, B. A. Bahr, X. Y. Bai, Y. Bailly, R. Baiocchi, G. Baldini, W. Balduini, A. Ballabio, B. A. Bamber, E. T. Bampton, G. +. Juh+ísz, C. R. Bartholomew, D. C. Bassham, R. C. Bast, H. Batoko, B. H. Bay, I. Beau, D. M. B+®chet, T. J. Begley, C. Behl, C. Behrends, S. Bekri, B. Bellaire, L. J. Bendall, L. Benetti, L. Berliocchi, H. Bernardi, F. Bernassola, S. +. Besteiro, I. Bhatia-Kissova, X. Bi, M. Biard-Piechaczyk, J. S. Blum, L. H. Boise, P. Bonaldo, D.

ACCEPTED MANUSCRIPT

L. Boone, B. C. Bornhauser, K. R. Bortoluci, I. Bossis, F. d. r. Bost, J. P. Bourquin, P. Boya, M. l. Boyer-Guittaut, P. V. Bozhkov, N. R. Brady, C. Brancolini, A. Brech, J. E. Brenman, A. Brennand, E. H. Bresnick, P. Brest, D. Bridges, M. L. Bristol, P. S. Brookes, E. J. Brown, J. H. Brumell, N. Brunetti-Pierri, U. T. Brunk, D. E. Bulman, S. J. Bultman, G. Bultynck, L. F. Burbulla, W. Bursch, J. P. Butchar, W. Buzgariu, S. P. Bydlowski, K. Cadwell, M. Cahov+í, D. Cai, J. Cai, Q. Cai, B. Calabretta, J. Calvo-Garrido, N. Camougrand, M. Campanella, J. Campos-Salinas, E. Candi, L. Cao, A. B. Caplan, S. R. Carding, S. M. Cardoso, J. S. Carew, C. R. Carlin, V. Carmignac, L. A. Carneiro, S. Carra, R. A. Caruso, G. Casari, C. Casas, R. Castino, E. Cebollero, F. Cecconi, J. Celli, H. Chaachouay, H. J. Chae, C. Y. Chai, D. C. Chan, E. Y. Chan, R. C.-C. Chang, C. M. Che, C. C. Chen, G. C. Chen, G. Q. Chen, M. Chen, Q. Chen, S. S. L. Chen, W. Chen, X. Chen, X. Chen, X. Chen, Y. G. Chen, Y. Chen, Y. Chen, Y. J. Chen, Z. Chen, A. Cheng, C. H. Cheng, Y. Cheng, H. Cheong, J. H. Cheong, S. Cherry, R. Chess-Williams, Z. H. Cheung, E. Chevet, H. L. Chiang, R. Chiarelli, T. Chiba, L. S. Chin, S. H. Chiou, F. V. Chisari, C. H. Cho, D. H. Cho, A. M. Choi, D. Choi, K. S. Choi, M. E. Choi, S. Chouaib, D. Choubey, V. Choubey, C. T. Chu, T. H. Chuang, S. H. Chueh, T. Chun, Y. J. Chwae, M. L. Chye, R. Ciarcia, M. R. Ciriolo, M. J. Clague, R. S. Clark, P. G. Clarke, R. Clarke, P. Codogno, H. A. Coller, M. a. I. Colombo, S. Comincini, M. Condello, F. Condorelli, M. R. Cookson, G. H. Coombs, I. Coppens, R. Corbalan, P. Cossart, P. Costelli, S. Costes, A. Coto-Montes, E. Couve, F. P. Coxon, J. M. Cregg, J. L. Crespo, M. J. Cronj+®, A. M. Cuervo, J. J. Cullen, M. J. Czaja, M. D'Amelio, A. Darfeuille-Michaud, L. M. Davids, F. E. Davies, M. De Felici, J. F. de Groot, C. A. de Haan, L. De Martino, A. De Milito, V. De Tata, J. Debnath, A. Degterev, B. Dehay, L. M. Delbridge, F. Demarchi, Y. Z. Deng, J. +. Dengjel, P. Dent, D. Denton, V. Deretic, S. D. Desai, R. J. Devenish, M. Di Gioacchino, G. Di Paolo, C. Di Pietro, G. D+¡az-Araya, I. s. D+¡az-Laviada, M. T. Diaz-Meco, J. Diaz-Nido, I. Dikic, S. P. Dinesh-Kumar, W. X. Ding, C. W. Distelhorst, A. Diwan, M. Djavaheri-Mergny, S. Dokudovskaya, Z. Dong, F. C. Dorsey**.** 2012**.** Guidelines for the use and interpretation of assays for monitoring autophagy. Autophagy 8, 445-544.

Komatsu, M., S. Waguri, T. Chiba, S. Murata, J. i. Iwata, I. Tanida, T. Ueno, M. Koike, Y. Uchiyama, E. Kominami, K. Tanaka**.** 2006**.** Loss of autophagy in the central nervous system causes neurodegeneration in mice. Nature 441, 880-884.

Komatsu, M., S. Waguri, M. Koike, Y. s. Sou, T. Ueno, T. Hara, N. Mizushima, J. i. Iwata, J. Ezaki, S. Murata, J. Hamazaki, Y. Nishito, S. i. Iemura, T. Natsume, T. Yanagawa, J. Uwayama, E. Warabi, H. Yoshida, T. Ishii, A. Kobayashi, M. Yamamoto, Z. Yue, Y. Uchiyama, E. Kominami, K. Tanaka**.** 2007a**.** Homeostatic Levels of p62 Control Cytoplasmic Inclusion Body Formation in Autophagy-Deficient Mice. Cell 131, 1149-1163.

Komatsu, M., Q. J. Wang, G. R. Holstein, V. L. Friedrich, J. i. Iwata, E. Kominami, B. T. Chait, K. Tanaka, Z. Yue**.** 2007b**.** Essential role for autophagy protein Atg7 in the maintenance of axonal homeostasis and the prevention of axonal degeneration. Proc. Natl. Acad .Sci. U S A.104, 14489-14494.

Lambert de Rouvroit, C. and A. M. Goffinet**.** 1998**.** The reeler mouse as a model of brain development. Adv. Anat. Embryol. Cell Biol. 150, 1-106.

Landis, D. M. D. and R. L. Sidman**.** 1978**.** Electron microscopic analysis of postnatal histogenesis in the cerebellar cortex of staggerer mutant mice. J. Comp. Neurol. 179, 831-864.

Landis, S. C. 1973**.** Ultrastructural changes in the mitochondria of the cerebellar Purkinje cells of nervous mutant mice. J Cell Biol. 57, 782-797.

Lee, J. A., A. Beigneux, S. T. Ahmad, S. G. Young, F. B. Gao**.** 2007**.** ESCRT-III Dysfunction Causes Autophagosome Accumulation and Neurodegeneration. Curr. Biol. 17, 1561-1567.

Lewis, P. D. 1975**.** Cell death in the germinal layers of the postnatal rat brain. Neuropathol. Appl. Neurobiol. 1, 21-29.

Li, J., L. Yu, X. Gu, Y. Ma, R. Pasqualini, W. Arap, E. Y. Snyder, R. L. Sidman**.** 2013**.** Tissue plasminogen activator regulates Purkinje neuron development and survival. Proc Natl. Acad. Sci. U S A. 110, 2410-2419.

ACCEPTED MANUSCRIPT

Liberski, P. P., D. R. Brown, B. Sikorska, B. Caughey, P. Brown. 2008. Cell death and autophagy in prion diseases (transmissible spongiform encephalopathies). Folia Neuropathol. 46, 1-25.

Lossi, L., C. Castagna, and A. Merighi. (2015). Neuronal Cell Death: An Overview of Its Different Forms in Central and Peripheral Neurons, pp. 1-18 *In L. Lossi and A. Merighi* [eds.], Neuronal Cell Death. (Springer New York,).

Lossi, L. and G. Gambino. 2008. Apoptosis of the cerebellar neurons. Histol. Histopathol. 23, 367-380.

Lossi, L., G. Gambino, C. Salio, A. Merighi. 2010. Autophagy regulates the post-translational cleavage of BCL-2 and promotes neuronal survival. Scientific World Journal. 10, 924-929.

Lossi, L. and A. Merighi. 2003. In vivo cellular and molecular mechanisms of neuronal apoptosis in the mammalian CNS. Progr. Neurobiol. 69, 287-312.

Lossi, L., S. Mioletti, A. Merighi. 2002. Synapse-independent and synapse-dependent apoptosis of cerebellar granule cells in postnatal rabbits occur at two subsequent but partly overlapping developmental stages. Neurosci. 112, 509-523.

Lossi, L., I. Tamagno, A. Merighi. 2004. Molecular morphology of neuronal apoptosis: activation of caspase 3 during postnatal development of mouse cerebellar cortex. J. Mol. Histol. 35, 621-629.

Maiuri, M. C., E. Zalckvar, A. Kimchi, G. Kroemer. 2007. Self-eating and self-killing: crosstalk between autophagy and apoptosis. Nat. Rev. Mol Cell Biol 8, 741-752.

Mariani, J., F. Crepel, K. Mikoshiba, J. P. Changeux, C. Sotelo. 1977. Anatomical, Physiological and Biochemical Studies of the Cerebellum from Reeler Mutant Mouse. Phil. Trans Royal Soc. Lon. B. 281, 1-28.

Martin, L. J., F. E. Sieber, R. J. Traystman. 2000. Apoptosis and Necrosis Occur in Separate Neuronal Populations in Hippocampus and Cerebellum After Ischemia and Are Associated With Differential Alterations in Metabotropic Glutamate Receptor Signaling Pathways. J Cereb. Blood Flow Metab. 20, 153-167.

Marzban, H., M. R. Del Bigio, J. Alizadeh, S. Ghavami, R. M. Zachariah, M. Rastegar. 2015. Cellular commitment in the developing cerebellum. Front .Cell. Neurosci. 8, 450

Migheli, A., A. Attanasio, W. H. Lee, S. A. Bayer, B. Ghetti. 1995. Detection of apoptosis in weaver cerebellum by electron microscopic in situ end-labeling of fragmented DNA. Neurosci. Lett. 199, 53-56.

Migheli, A., R. Piva, J. Wei, A. Attanasio, S. Casolino, M. E. Hodes, S. R. Dlouhy, S. A. Bayer, B. Ghetti. 1997. Diverse cell death pathways result from a single missense mutation in weaver mouse Am.J.Pathol. 151, 1629-1638.

Mikoshiba, K., K. Nagaike, S. Kohsaka, K. Takamatsu, E. Aoki, Y. Tsukada. 1980. Developmental studies on the cerebellum from reeler mutant mouse in vivo and in vitro. Develop. Biol. 79, 64-80.

Moreno, S., V. Imbroglini, E. Ferraro, C. Bernardi, A. Romagnoli, A. Berrebi, F. Cecconi. 2006. Apoptosome impairment during development results in activation of an autophagy program in cerebral cortex. Apoptosis 11, 1595-1602.

Nishiyama, J. and M. Yuzaki. 2010. Excitotoxicity and autophagy: Lurcher may not be a model of "autophagic cell death". Autophagy 6, 568-570.

Nixon, R. A. 2013. The role of autophagy in neurodegenerative disease. Nat. Med. 19, 983-997.

Accepted Manuscript

ACCEPTED MANUSCRIPT

Norman, D. J., L. Feng, S. S. Cheng, J. Gubbay, E. Chan, N. Heintz. 1995. The lurcher gene induces apoptotic death in cerebellar Purkinje cells. Development 121, 1183-1193.

Pamenter, M. E., G. A. Perkins, A. K. McGinness, X. Q. Gu, M. H. Ellisman, G. G. Haddad. 2012. Autophagy and apoptosis are differentially induced in neurons and astrocytes treated with an in vitro mimic of the ischemic penumbra. PLoS. One. 7, 51469.

Patil, N., D. R. Cox, D. Bhat, M. Faham, R. M. Myers, A. S. Peterson. 1995. A potassium channel mutation in weaver mice implicates membrane excitability in granule cell differentiation. Nat. Genet. 11, 126-129.

Phillips, R. J. S. 1960. "Lurcher", a new gene in linkage group XI of the house mouse. J. Genet. 57, 35-42.

Rakic, P. and R. L. Sidman. 1973. Weaver Mutant Mouse Cerebellum: Defective Neuronal Migration Secondary to Abnormality of Bergmann Glia. Proc. Natl. Acad. Sci. U S A 70, 240-244.

Rami, A. 2009. Review: autophagy in neurodegeneration: firefighter and/or incendiarist? Neuropathol. Appl. Neurobiol. 35, 449-461.

Schweichel, J. U. and H. J. Merker. 1973. The morphology of various types of cell death in prenatal tissues. Teratology 7, 253-266.

Sidman, R. L., P. W. Lake, M. M. Dickie. 1962. Staggerer, a new mutation in the mouse affecting the cerebellum. Science 137, 610-612.

Smeyne, R. J. and D. Goldowitz. 1989. Development and death of external granular layer cells in the weaver mouse cerebellum: a quantitative study. J. Neurosci. 9, 1608-1620.

Smeyne, R. J. and D. Goldowitz. 1990. Purkinje cell loss is due to a direct action of the weaver gene in Purkinje cells: evidence from chimeric mice. Brain Res. Dev. Brain Res. 52, 211-218.

Tomoda, T., R. S. Bhatt, H. Kuroyanagi, T. Shirasawa, M. E. Hatten. 1999. A mouse serine/threonine kinase homologous to C. elegans UNC51 functions in parallel fiber formation of cerebellar granule neurons. Neuron 24, 833-846.

Triarhou, L. C. 2010. Biological clues on neuronal degeneration based on theoretical fits of decay patterns: towards a mathematical neuropathology. Folia Neuropathol. 48, 3-10.

Wei, L., B. H. Han, Y. Li, C. L. Keogh, D. M. Holtzman, S. P. Yu. 2006. Cell death mechanism and protective effect of erythropoietin after focal ischemia in the whisker-barrel cortex of neonatal rats. J. Pharmacol. Exp. Ther. 317, 109-116.

Won, S. J., S. H. Kim, L. Xie, Y. Wang, X. O. Mao, K. Jin, D. A. Greenberg. 2006. Reelin-deficient mice show impaired neurogenesis and increased stroke size. Exp. Neurol. 198, 250-259.

Wood, K. A., B. Dipasquale, R. J. Youle. 1993. In situ labeling of granule cells for apoptosis-associated DNA fragmentation reveals different mechanisms of cell loss in developing cerebellum. Neuron 11, 621-632.

Yamaguchi, Y. and M. Miura. 2015. Programmed cell death in neurodevelopment. Dev. Cell 32, 478-490.

Yang, D. S., A. Kumar, P. Stavrides, J. Peterson, C. M. Peterhoff, M. Pawlik, E. Levy, A. M. Cataldo, R. A. Nixon. 2008. Neuronal apoptosis and autophagy cross talk in aging PS/APP Mice, a model of Alzheimer's disease. Am. J. Pathol. 173, 665-681.

Yuasa, S., J. Kitoh, S. Oda, K. Kawamura. 1993. Obstructed migration of Purkinje cells in the developing cerebellum of the reeler mutant mouse. Anat. Embryol. (Berl) 188, 317-329.

Accepted Manuscript

ACCEPTED MANUSCRIPT

Yue, Z. 2010. Autophagy in lurcher mice: indicted but yet to be acquitted for the death of Purkinje cells. Autophagy 6, 571-572.

Yue, Z., A. Horton, M. Bravin, P. L. DeJager, F. Selimi, N. Heintz. 2002. A Novel Protein Complex Linking the +¦2 Glutamate Receptor and Autophagy: Implications for Neurodegeneration in Lurcher Mice. Neuron 35, 921-933.

Zuo, J., P. L. De Jager, K. A. Takahashi, W. Jiang, D. J. Linden, N. Heintz. 1997. Neurodegeneration in Lurcher mice caused by mutation in [delta]2 glutamate receptor gene. Nature 388, 769-773.

Accepted Manuscript

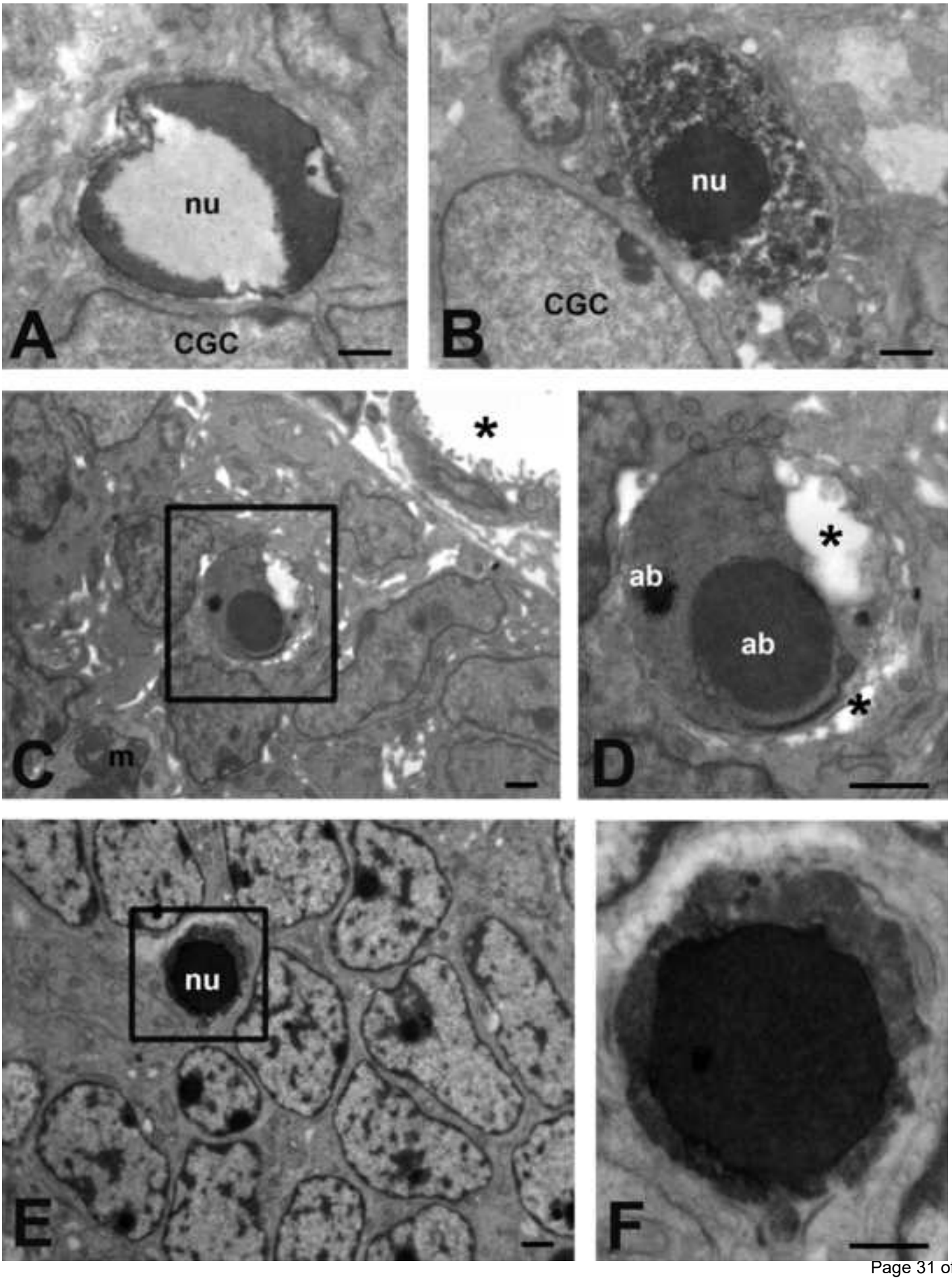
nu
A
CGC
nu
B
CGC
*
C
m
*
ab
ab
*
D
nu
E
F

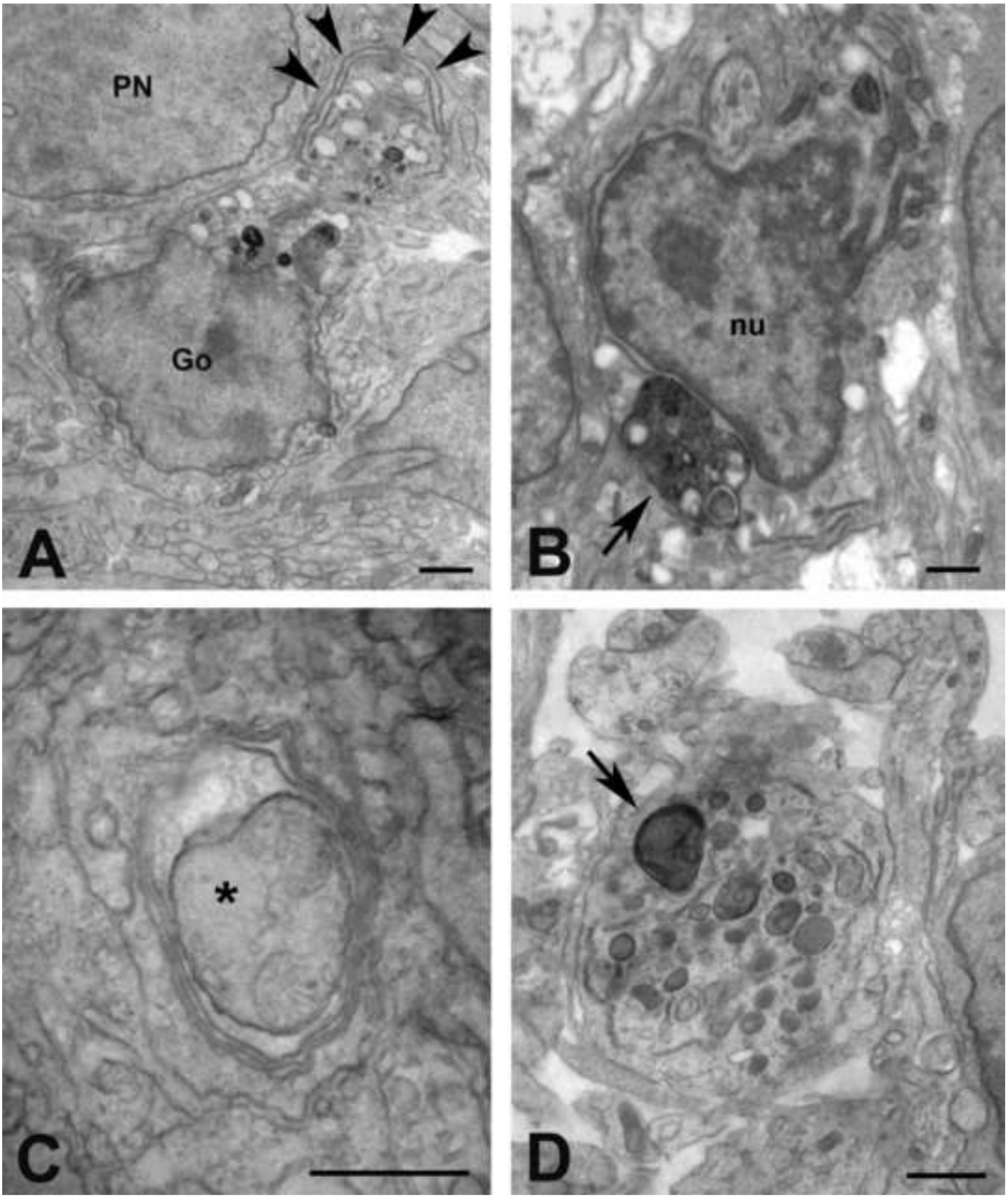
PN
Go
A
nu
B
*
C
D

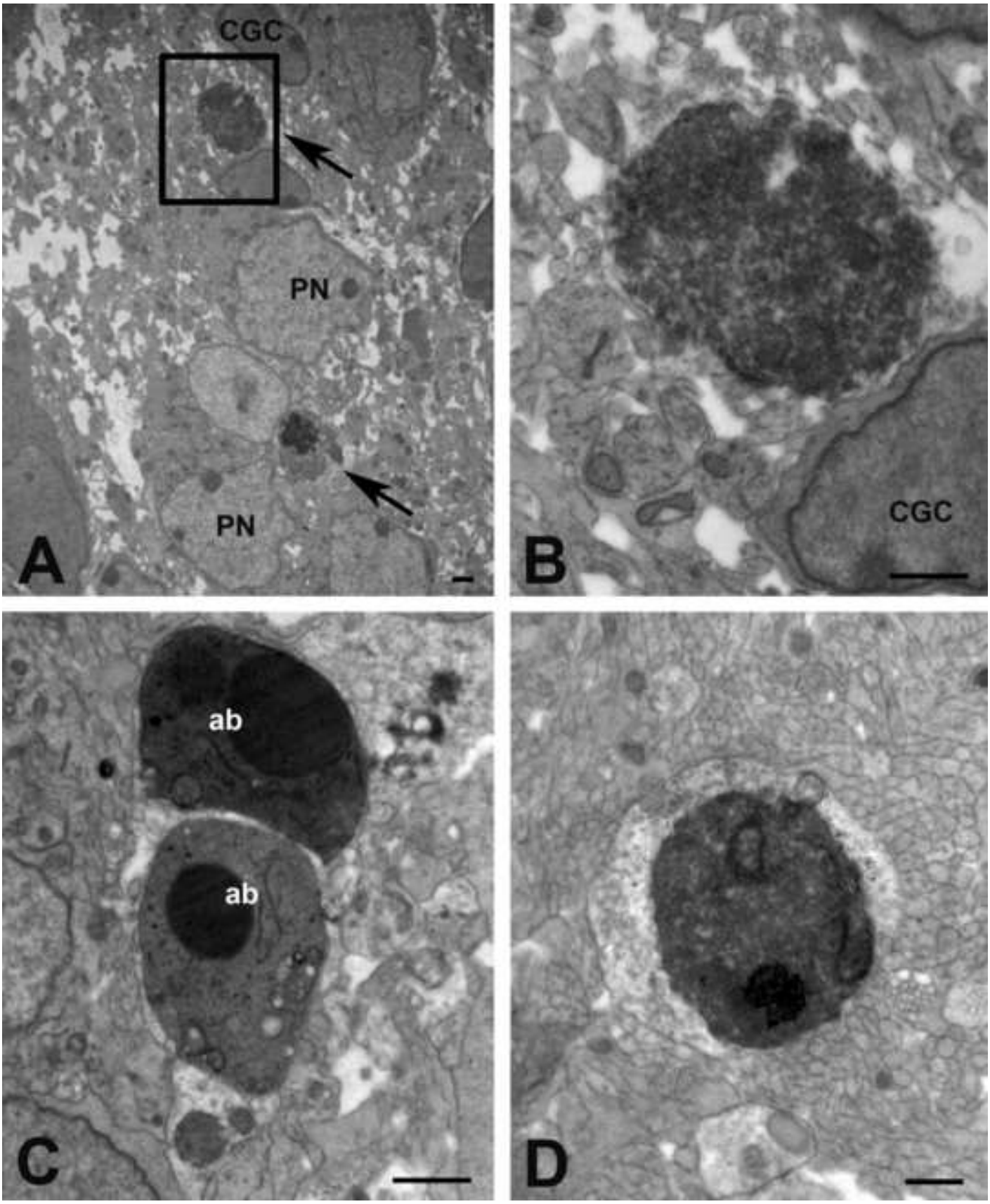
CGC
PN
PN
A
B
CGC
ab
ab
C
D

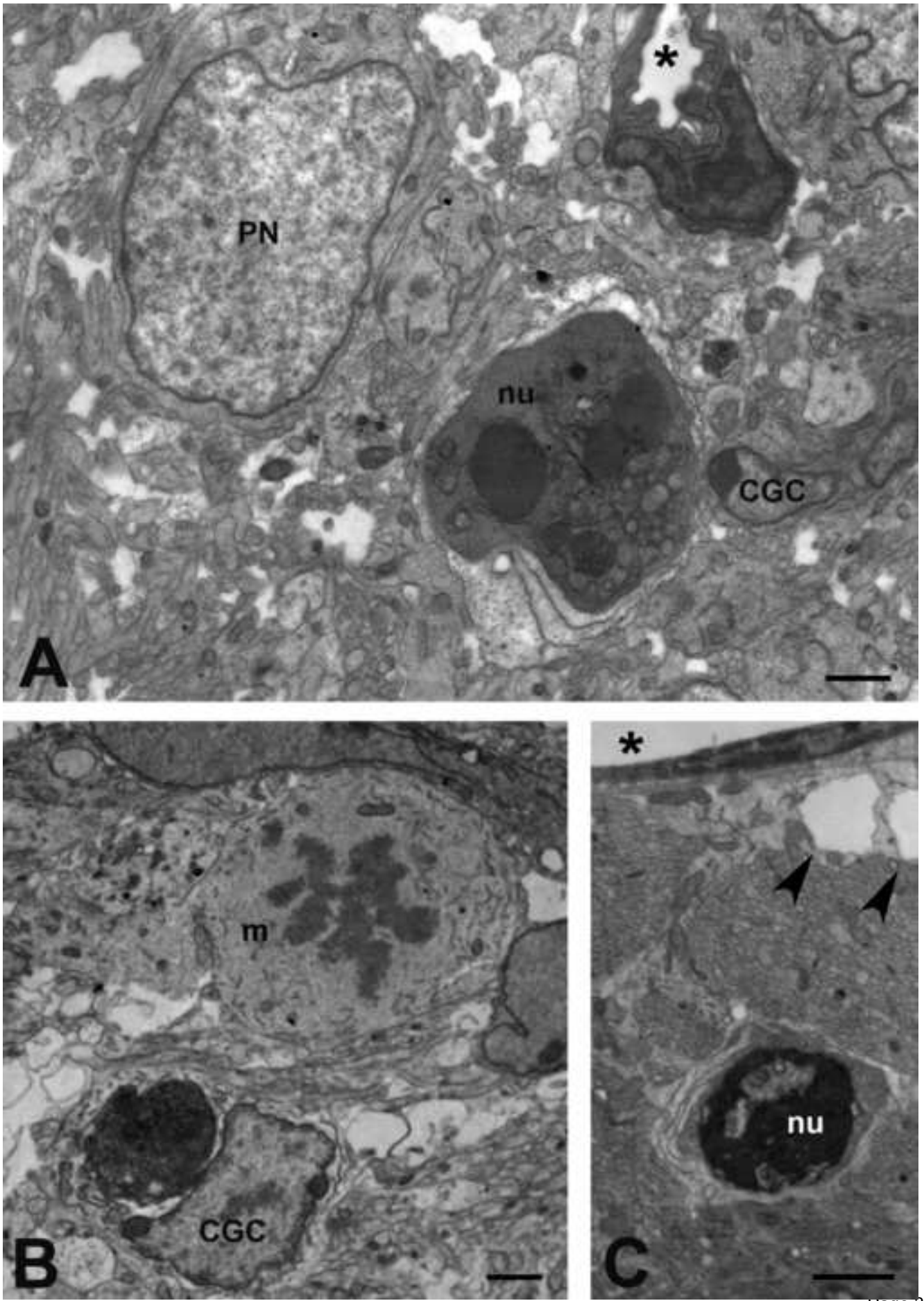
PN
*
nu
CGC
A
m
CGC
B
*
nu
C

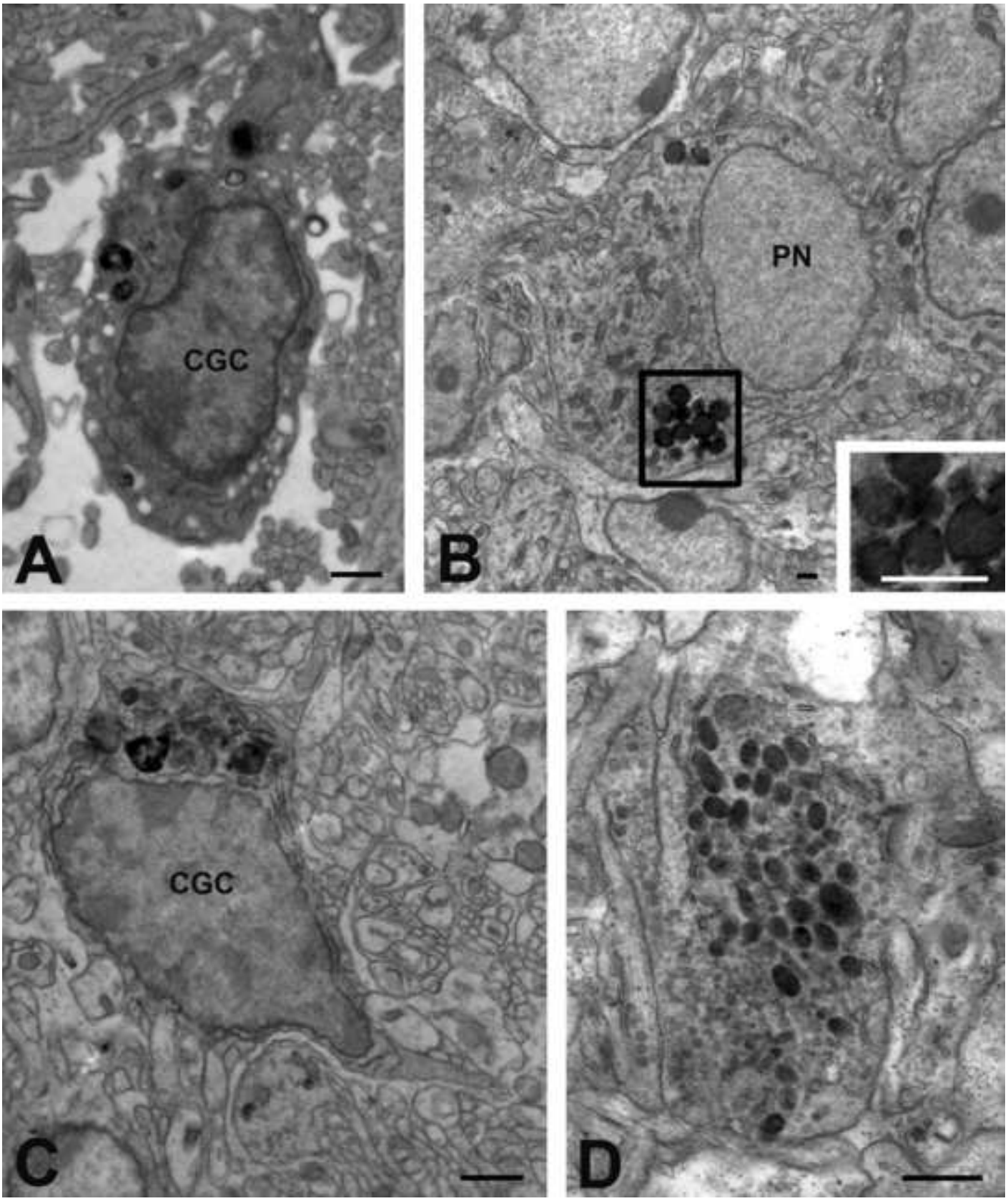
CGC
A
PN
B
CGC
C
D

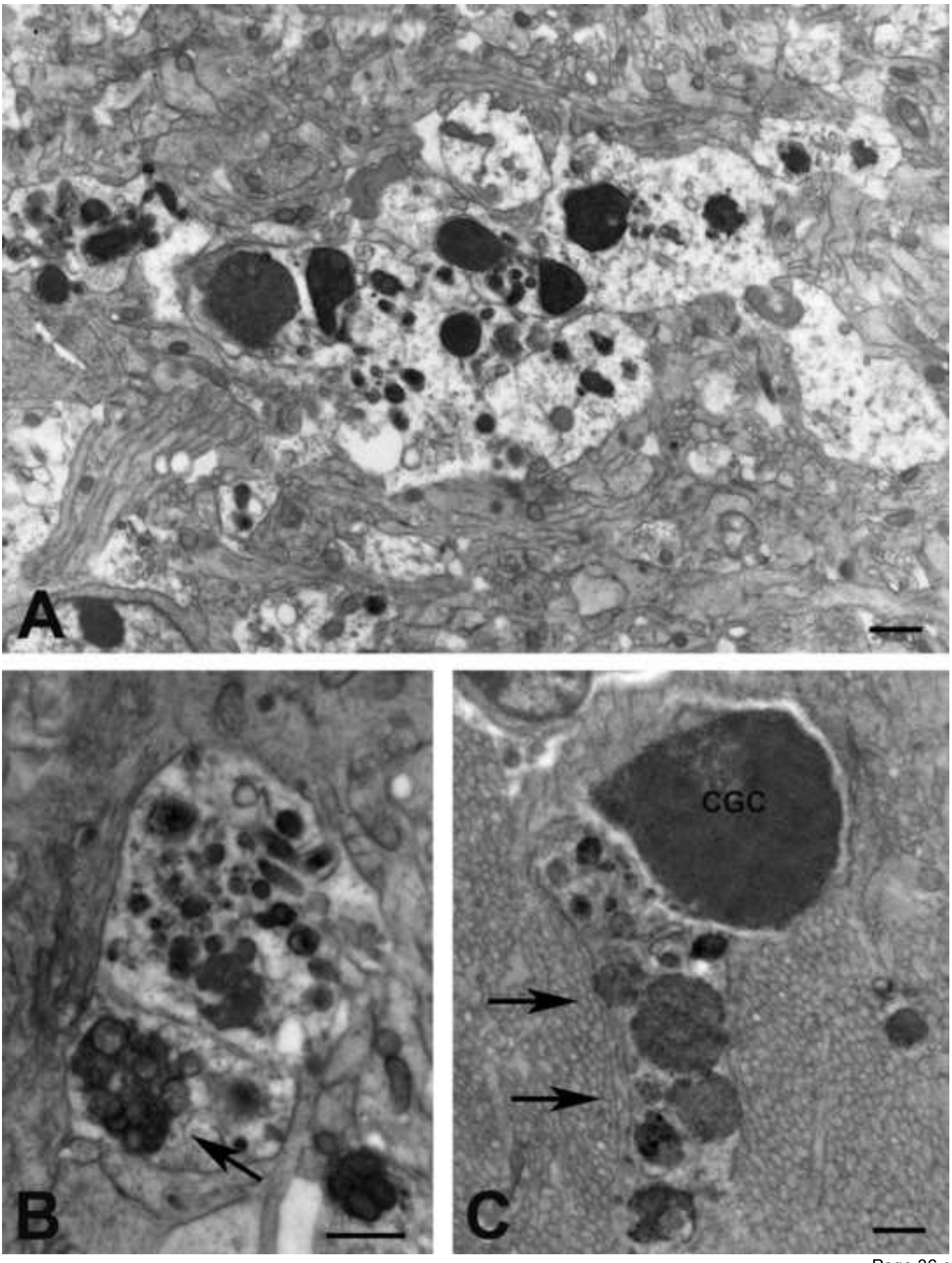
A
B
C
CGC

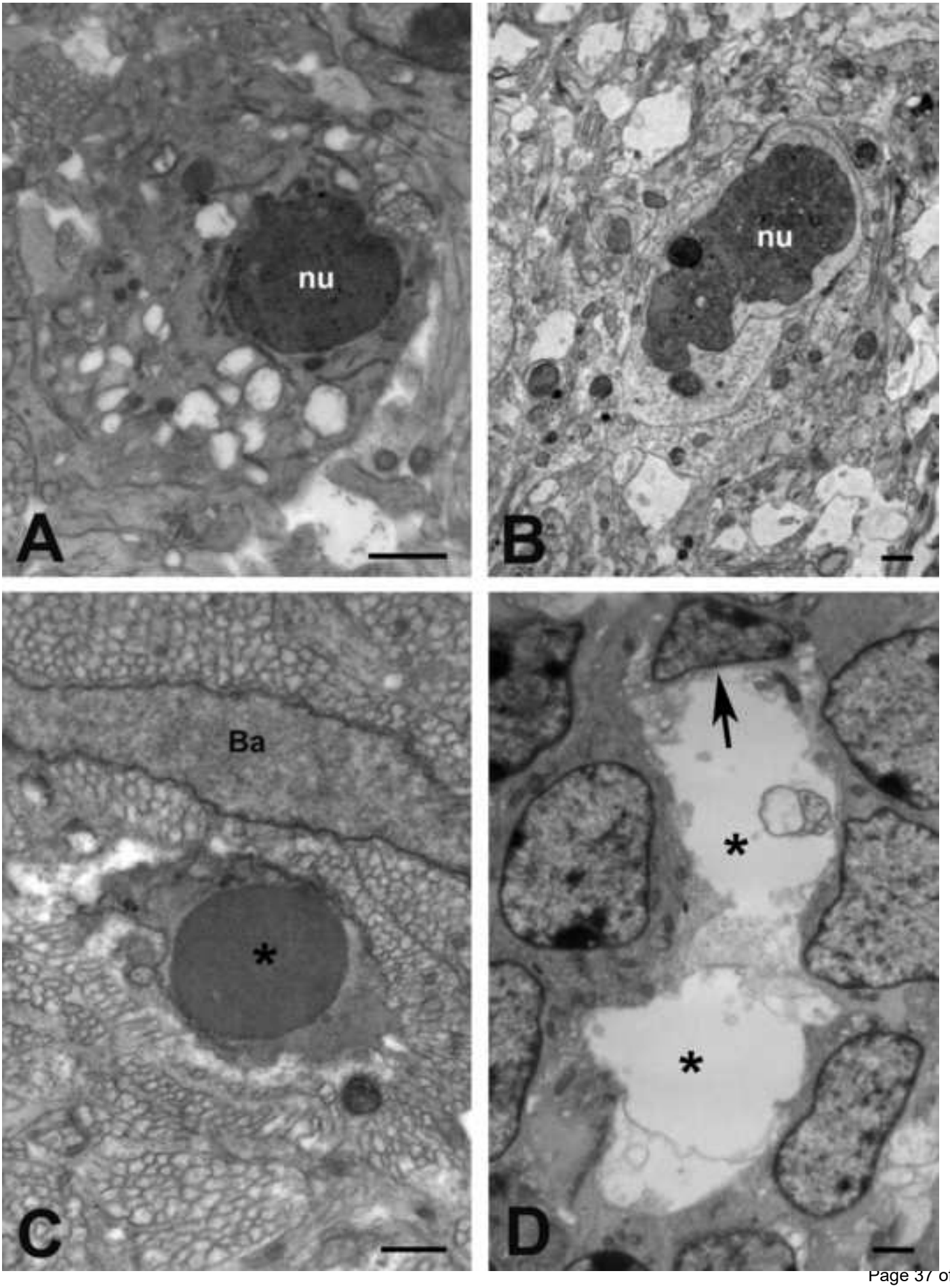
nu
A
nu
B
Ba
*
C
*
*
D

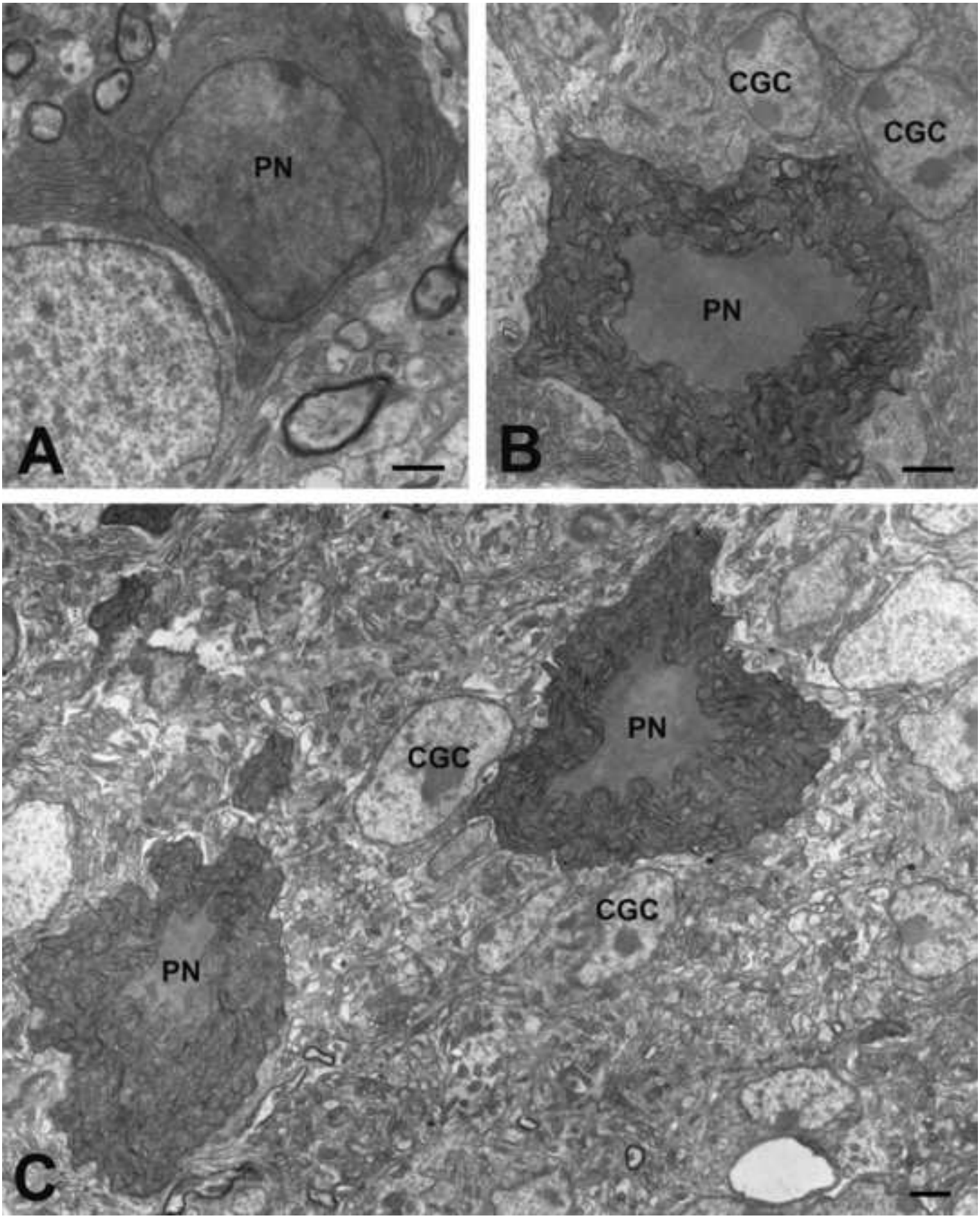
PN
A
CGC
CGC
PN
B
PN
CGC
CGC
PN
C